JOURNAL OF BACTERIOLOGY, Oct. 1992, p. 6624–6633
0021-9193/92/206624-10$02.00/0

Vol. 174, No. 20

AlgR-Binding Sites within the *algD* Promoter Make Up a Set of Inverted Repeats Separated by a Large Intervening Segment of DNA

C. D. MOHR, J. H. J. LEVEAU, D. P. KRIEG, N. S. HIBLER, AND V. DERETIC*

Department of Microbiology, University of Texas Health Science Center at San Antonio, San Antonio, Texas 78284-7758

Received 27 May 1992/Accepted 15 August 1992

Activation of *algD* by AlgR is essential for mucoidy, a virulence factor expressed by *Pseudomonas aeruginosa* in cystic fibrosis. Two AlgR-binding sites, RB1 and RB2, located far upstream from the *algD* mRNA start site, are essential for the high-level activity of *algD*. However, the removal of RB1 and RB2 does not completely abolish inducibility of *algD* in response to environmental signals. In this work, a third binding site for AlgR, termed RB3, near the *algD* mRNA start site was characterized. Deletion of RB3 abrogated both the AlgR-binding ability and the residual inducibility of the *algD* promoter. DNase I footprinting analysis of RB3 resulted in a protection pattern spanning nucleotides −50 to −30. Eight of 10 residues encompassing a continuous region of protection within RB3 (positions −45 to −36) matched in the inverted orientation the conserved core sequence (ACCGTTCGTC) of RB1 and RB2. Quantitative binding measurements of AlgR association with RB1, RB2, and RB3 indicated that AlgR had significantly lower affinity for RB3 than for RB1 and RB2, with differences in the free energy of binding of 1.05 and 0.93 kcal/mol (4.39 and 3.89 kJ/mmol), respectively. Altering the core of RB2 to match the core of RB3 significantly reduced AlgR binding. Conversely, changing the core of RB3 to perfectly match the core of RB2 (mutant site termed RB3*) improved AlgR binding, approximating the affinity of RB2. RB3*, in the absence of the far upstream sites, showed an increase in activity, approaching the levels observed with the full-size *algD* promoter. Changing 4 nucleotides in two different combinations within the core of RB3 abolished the binding of AlgR to this site and resulted in a significant reduction of promoter activity in the presence of the far upstream sites. Thus, (i) the core sequence is essential for AlgR binding; (ii) the three binding sites, RB1, RB2, and RB3, are organized as an uneven palindrome with symmetrical sequences separated by 341 and 417 bp; and (iii) all three sites participate in *algD* activation.

Pseudomonas aeruginosa is the major pathogen infecting the lungs of cystic fibrosis patients (18, 19). Among its arsenal of virulence factors is the ability to synthesize and secrete the exopolysaccharide alginate (14, 18, 27, 31). The overproduction of alginate by cells results in mucoid colony morphology, a frequently observed trait among cystic fibrosis isolates. The role of mucoidy in sustained bacterial colonization and chronic infection of the cystic fibrosis lung has been established in numerous studies (18, 19, 32). The emergence and persistence of mucoid *P. aeruginosa* in cystic fibrosis are underlying causes of the progressive lung damage and mortality associated with this disease (18, 19).

A key step in the overproduction of alginate and the establishment of mucoidy is the strong transcriptional activation of the *algD* gene encoding GDPmannose dehydrogenase (8–10, 30). This enzyme catalyzes the oxidation of GDPmannose into GDPmannuronic acid, a direct precursor of alginate (8, 33). The *algD* promoter is subject to complex transcriptional regulation and has become a benchmark for monitoring molecular events which govern expression of the alginate system (10, 15, 17, 39). One of the regulatory elements (12–14, 21, 39) positively controlling *algD* is AlgR (9), a response regulator from a superfamily of bacterial signal transduction systems (7). Insertional inactivation of *algR* renders cells nonmucoid and dramatically affects transcription of *algD* by reducing the *algD* promoter activity approximately 100-fold (30). The recent purification of AlgR has allowed demonstration of its direct interaction with the *algD* promoter (21, 29). It has been shown that AlgR binds to two sites far upstream from the *algD* mRNA start site (Fig. 1). These binding sites, designated RB1 and RB2 (29), span nucleotides −479 to −457 and −400 to −380, respectively, relative to the *algD* mRNA start site (29). RB1 and RB2 are located in the region (Fig. 1, FUS [for far upstream sites]) identified in this laboratory, by deletion and functional analyses, as critical for the high-level transcription of *algD* (30). Centered around the middle of both RB1 and RB2 is a perfectly conserved 10-bp sequence (5′ACCGTTCGTC3′) termed the core region (29). The core sequences of RB1 and RB2 form a pair of direct repeats with a head-to-tail separation of 66 nucleotides (29, 30).

When RB1 and RB2 are sequentially deleted, this results in a stepwise reduction of *algD* transcription; however, the promoter is still responsive to induction (30). The reasons for this residual activity are currently unknown. In the process of characterizing the high-affinity AlgR-binding sites RB1 and RB2, we observed a relatively weak but specific interaction of AlgR with sequences closer than RB1 and RB2 to the *algD* mRNA start site. This putative lower-affinity binding site(s) appeared to be separated from the far upstream sites RB1 and RB2 by a long region of DNA not binding AlgR. In this study, we demonstrate that AlgR does bind close to the *algD* mRNA start site, report a precise definition of this third discrete AlgR-binding site within the *algD* promoter, establish the role of the core sequence for AlgR binding, and demonstrate participation of all three binding sites in *algD* activation.

* Corresponding author.

MATERIALS AND METHODS

Growth conditions, bacterial strains, DNA constructs, recombinant DNA methods, and transcriptional fusion studies. The medium used for growing all *Escherichia coli* strains was LB, supplemented with 40 μg of ampicillin per ml and 30 μg of chloramphenicol per ml, when required. Protein overexpression was performed in *E. coli* BL21(DE3) harboring pLysS (36). The plasmid constructs used for the overexpression and purification of AlgR have been described previously (29). DNA manipulations were done according to published procedures (1). DNA was sequenced by the dideoxy-chain termination method with modifications as described previously (24). The nucleotide sequence of the *algD* promoter from a PAO strain has been published previously (GenBank accession number M37205) (30). Templates for DNA sequencing and for generating uniformly labeled probes used in quantitative binding measurements were made from the previously published *algD* deletion clones in M13 (30). The plasmids used to generate end-labeled probes for gel mobility shift assays and DNase I footprinting analysis were constructed by subcloning deletion derivatives of the *algD* promoter from PAO (30) into pUC12 as *Hin*dIII-*Eco*RI fragments. For transcriptional fusion studies, appropriate DNA fragments were cloned into the transcriptional fusion vector pVDX18 and conjugated into *P. aeruginosa* PAO568 (*muc-2*), and exconjugants were selected on *Pseudomonas* isolation agar (Difco) supplemented with carbenicillin (300 μg/ml). The media and growth conditions for induction with NaCl or alternative nitrogen sources (nitrate instead of ammonia) have been previously described (10, 30). Promoter activity was assayed by determining the activity of catechol 2,3-dioxygenase (CDO), the gene product of *xylE* used as a reporter gene, as previously described (10, 23, 30). One unit of CDO is defined as the amount of enzyme required to convert 1 μmol of catechol into 2-hydroxymuconic semialdehyde in 1 min at 24°C.

Oligonucleotide-mediated site-directed mutagenesis. The AlgR-binding sites (RB2 and RB3) were mutagenized applying two methods: (i) the in vitro selection procedure of Vandeyar et al. (38), based on incorporation of 5-methyl-dCTP in the mutant strand (using the T7-GEN in vitro mutagenesis kit from United States Biochemical); and (ii) the in vivo selection method of Bauer et al. (2), using M13 vectors with amber mutations. M13 DNA templates containing different deletions of the *algD* promoter and cloned native T7 DNA polymerase (lacking strand displacement activity) for primer extension reactions were used for both methods. Mutagenic oligonucleotides were (underlined residues indicate the residues different from the wild-type sequence): MO1 (5'ATTTCGCGAGCGGGACGAACGGT CGGAACTTCCCTC3'), MO3 (5'ATTTCGCGAGCGGGA CAAGTAACCGGAACTTCCCTC3'), MO4 (5'ATTTCGC GAGCGGGGTAGACGACCGGAACTTCCCTC3'), and MO5 (5'ATAGGCCTACTCGGCCGTTTGTCTGCAAGTCATTC G3'). To facilitate screening, the changes were designed so that a new restriction site was created or the existing one was lost. Mutations were confirmed by dideoxy sequencing, using a primer extending from positions −237 to −221 relative to the mRNA start site (5'GGTCGAAGATTAAG GAA3'; LO1) and the universal 17-bp primer.

Protein purification and analysis. The overexpression and purification of AlgR was performed as previously described (29). Protein concentration was determined by the Bradford assay (3). The purity of AlgR was over 90%, as judged by Coomassie blue stains and densitometry of sodium dodecyl sulfate (SDS)-polyacrylamide gels (29).

Mobility shift DNA binding assay. The DNA probes used for the mapping of RB3 by gel mobility shift assay were generated by digestion with *Cla*I (cutting at position +11 relative to the *algD* mRNA start site), treatment with phosphatase, and phosphorylation with [γ-^{32}P]ATP (6,000 Ci/mmol; DuPont NEN) catalyzed by polynucleotide kinase. Upon digestion with a second restriction endonuclease, the end-labeled fragments were gel purified. Probes (approximately 5×10^4 cpm) were incubated with different amounts of AlgR (7.8 to 331 ng) at 20°C for 10 min in a 10-μl reaction mixture containing 25 mM Tris-HCl (pH 8.0), 0.5 mM EDTA, 0.5 mM dithiothreitol, 20 mM KCl, 5% glycerol, and 10 μg of native salmon sperm DNA per ml. All reaction mixtures contained 0.25 μg of pUC12 as additional nonspecific competitor DNA. After incubation, the protein-DNA complexes and free DNA were separated on a 5% native polyacrylamide gel in a solution consisting of 6.7 mM Tris-HCl (pH 7.9), 3.3 mM sodium acetate, and 1 mM EDTA, as described previously (29). The gels were vacuum dried and autoradiographed.

DNase I footprinting analysis and localization of footprints by comparison with DNA sequence generated using dideoxynucleotide sequencing method. 5'-end-labeled probes were generated as described for mobility shift DNA binding assay. End-labeled fragments were generated by second digestion [with either *Nsi*I (−144) or *Eco*RV (−80)]. After incubation of 4×10^4 cpm of radiolabeled probe with either 1.5 or 3 μg of AlgR in the standard binding reaction mixture, the concentration of $MgCl_2$ was adjusted to 5 mM and 200 ng of DNase I was added. Following a second incubation for 1 min at room temperature, the reaction was stopped by the addition of an equal volume of a solution containing 1% SDS, 100 mM EDTA, 200 mM NaCl, and 2 mg/ml of tRNA, followed by phenol extraction and ethanol precipitation. The products of DNase I digestion were run on sequencing gels in parallel with a sequencing ladder generated using the 16-mer oligonucleotide primer MO2 (5'CGATAGGCAT CGCGGT3'). This oligonucleotide extended from positions +13 to −3 of the previously published *algD* promoter sequence (30), and its 5' end matched the labeled position within the probes used for DNase I footprinting analysis. Thus, the boundaries of RB3 were precisely determined by directly comparing the footprints with the sequencing ladder.

Quantitative binding measurements. Probes for quantitative binding studies were uniformly labeled with [α-^{32}P] dCTP (3,000 Ci/mmol; DuPont NEN) and Klenow fragment of DNA polymerase I. This was achieved by synthesizing the second strand on single-stranded templates from clones of the *algD* promoter in M13 primed by the universal 17-bp primer. The products were digested with appropriate enzymes, and double-stranded, labeled fragments were purified on polyacrylamide gels. These probes were labeled to high specific activities, permitting maintenance of a low DNA input (for RB2, 0.1 to 0.18 pmol; for RB3, 0.24 to 0.36 pmol) relative to AlgR concentrations in the binding reaction mixture. Protein-DNA binding, separation of products, and detection of the products were carried out as described for mobility shift DNA binding assay.

The autoradiograms were quantitatively analyzed using a two-dimensional scanner. Digitized film images were used to derive integrated optical densities of bands corrected for film background density. The integrated densities of free DNA were used to calculate the fraction of probe in protein-DNA

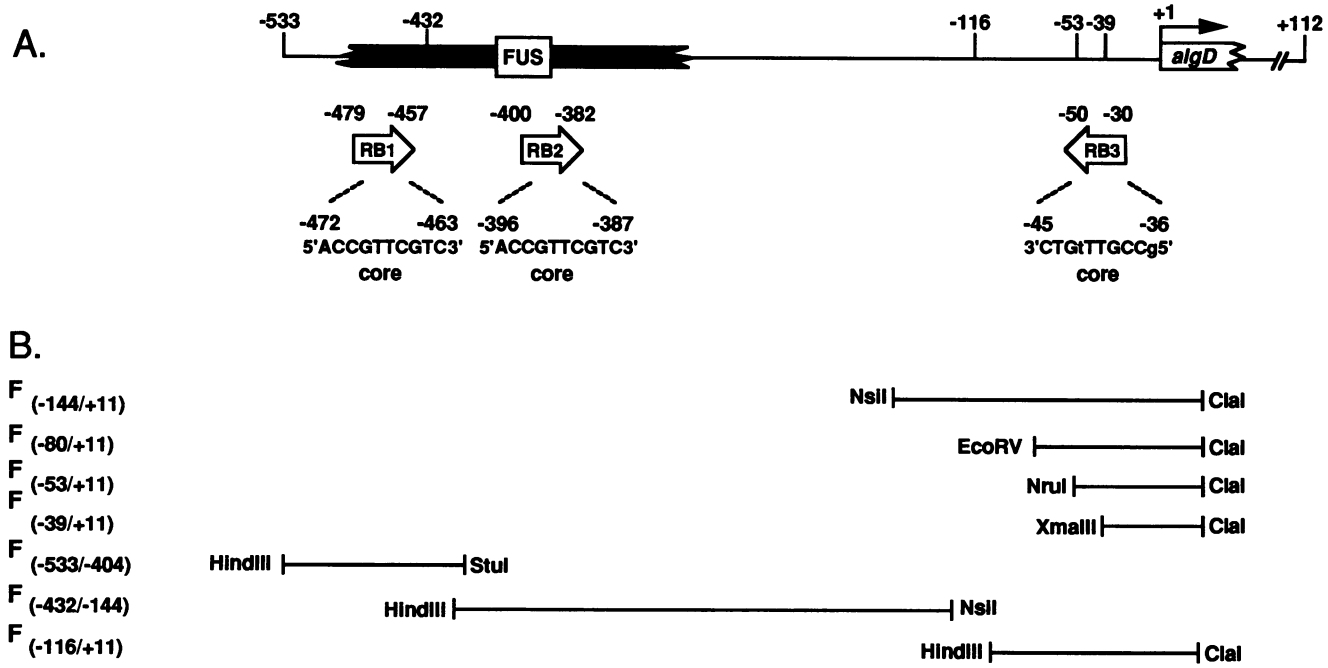

FIG. 1. (A) Organization of the AlgR-binding sites within the *algD* promoter. All numbers denoting nucleotide positions are given relative to the *algD* mRNA start site (+1; bent arrow). The solid black box represents the far upstream sites (FUS) previously identified as being required for the high-level transcription and environmental modulation of *algD* (30). RB1 and RB2 are the previously identified AlgR-binding sites (29). RB3 is the third AlgR-binding site identified and characterized in this study. Numbers above the boxes with arrowheads represent the limits of AlgR footprints. Numbers below the boxes correspond to the limits of the 10-bp core sequence shared by each binding site. Arrowheads on boxes labeled RB1, RB2, and RB3 indicate the orientations of the respective core sequences. Lowercase letters represent the two nucleotides in the RB3 core sequence not matching the corresponding nucleotides in the core of RB1 and RB2. Negative numbers above the line represent the positions of the 5′ ends of fragments used for expression studies; the other end of such fragments was the *Eco*RI site at +112. (B) Overlapping series of fragments of the *algD* promoter and other fragments used for binding of AlgR in this study. *Hin*dIII sites were introduced by deletion procedure (30). Numbers in subscripts indicate positions of the restriction sites used to generate the fragments.

complexes. These values, expressed as percent saturation, were plotted against the concentration of AlgR, and used to calculate apparent association constants (K_{app}). According to the familiar Langmuir isotherm applied to fractional saturation of DNA for a single binding site (5, 6), at 50% saturation $K_{app} = 1/[R]_{1/2}$ (5, 6, 16). K_{app} values were computed by fitting the data to a nonlinear model based on Langmuir isotherm ($Y = K_{app}[AlgR]/(1 + K_{app}[AlgR])$, using the Levenberg-Marquardt algorithm (26). Curve-fitting computations and plotting were done using Sigma Plot program (Jandel Scientific) on a Macintosh computer. A measure of the difference in free energies of AlgR-RB2 and AlgR-RB3 binding was calculated from ratios of respective K_{app} values by using the relationship $\Delta\Delta G = -RT(\ln K_{app}^{RB2}/K_{app}^{RB3})$. Since contributions of terms such as dilution during gel electrophoresis and AlgR specific activity cancel out in this equation (as long as the same AlgR preparation is used for comparisons), the derived differences in free energies of binding should be independent of such variables.

RESULTS

Localization of a third AlgR-binding site within the *algD* promoter using gel mobility shift DNA binding assay. The limits of the previously identified AlgR-binding sites, RB1 and RB2, were initially mapped by using deletion subclones of the *algD* promoter in gel mobility shift DNA binding assays (29). In the course of performing these experiments, we observed that a DNA fragment containing sequences closer to the *algD* mRNA start site (−332 to +11) also showed the capacity to bind AlgR in a manner clearly indicating a sequence-specific interaction (29). In order to precisely map the limits of this third binding site, a set of overlapping DNA fragments within the region −144 to +11 was generated (Fig. 1B). This was facilitated by the presence of single sites for *Nsi*I, *Eco*RV, *Nru*I, and *Xma*III, located in the vicinity of the *algD* mRNA start site (Fig. 1B). All fragments were end labeled with ^{32}P at the same end point (*Cla*I; +11). The resulting fragments were used in gel mobility shift DNA binding assays with different concentrations of purified AlgR. Fragments $F_{(-144/+11)}$, $F_{(-80/+11)}$, and $F_{(-53/+11)}$ all showed equal abilities to bind AlgR (Fig. 2). Each reaction mixture using these probes formed a single protein-DNA complex at both concentrations of AlgR used, indicating the presence of a single AlgR-binding site within each labeled fragment. However, when a fourth labeled fragment $F_{(-39/+11)}$ was used, the ability to bind AlgR was lost (Fig. 2). This fragment was unable to bind AlgR, even when the concentration of AlgR was increased fourfold (Fig. 2, $F_{(-39/+11)}$, lane 3). This fragment differs from the last one able to bind AlgR by only 14 bp. These results permitted fine mapping of the third AlgR binding site, called RB3, within the *algD* promoter. Unlike the far upstream binding sites RB1 and RB2, RB3 was located close to the *algD* mRNA start site. At least a portion of this site had to be within the region spanning nucleotides −53 to −39. Interestingly, the *Xma*III site, used to generate $F_{(-39/+11)}$, disrupted a sequence which showed the best match of all sequences within

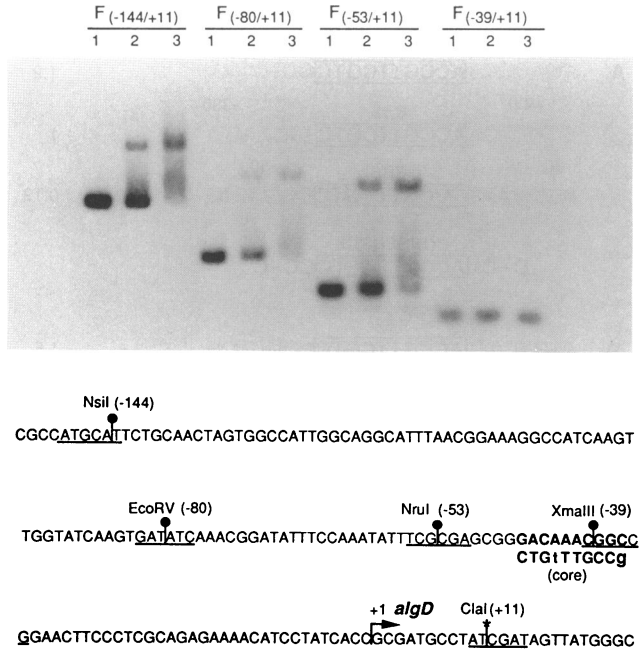

FIG. 2. Mapping of the third AlgR-binding site RB3 using a series of consecutively smaller fragments of the *algD* promoter. Shown is a mobility shift DNA binding assay performed as described in Materials and Methods. Four fragments $F_{(-144/+11)}$, $F_{(-80/+11)}$, $F_{(-53/+11)}$, and $F_{(-39/+11)}$ were generated by cleavage at the restriction sites *Nsi*I, *Eco*RV, *Nru*I, and *Xma*III, respectively. Each fragment was radiolabeled with ^{32}P (asterisk) at the common endpoint *Cla*I (+11). Lanes in each set: 1, radiolabeled fragment alone; 2, 80 ng of AlgR; 3, 330 ng of AlgR. Below the autoradiogram is the nucleotide sequence of the region immediately upstream of the *algD* mRNA start site (30). Numbers in parentheses are given relative to the *algD* mRNA start site. Underlined nucleotides are the restriction enzyme recognition sites. Black balloons denote cleavage sites. Bold nucleotides indicate the sequence (shown as double-stranded DNA) matching the 10-bp core sequence of the previously identified AlgR-binding sites RB1 and RB2. Other symbols are as described in the legend to Fig. 1.

the *algD* promoter to the 10-bp core sequence of RB1 and RB2 (Fig. 2).

Deletion of RB3 abrogates residual inducibility of the *algD* promoter observable in the absence of the far upstream sites RB1 and RB2. To examine whether AlgR binding at RB3 plays a role in *algD* activation in vivo, we used two DNA fragments extending from the *Nru*I (−53; with RB3) or *Xma*III (−39; without RB3) site and both ending at the *Eco*RI site located at position +112 relative to the *algD* mRNA start site. These fragments were cloned in the transcriptional fusion vector pVDX18, and promoter activity was assayed by following the procedures and growth conditions that had been previously used to functionally characterize the far upstream binding sites RB1 and RB2 (30). The results shown in Table 1 demonstrate that deletion of RB3 abrogates the residual activity and inducibility of this minimal *algD* promoter (*P* values using *t* test statistical analysis were below 0.002). Conditions inducing mucoidy and *algD* transcription in PAO568 (addition of salt to LB medium or growth on nitrate instead of ammonia as the nitrogen source) (10, 30) caused increased transcription of the fragment containing RB3 [Table 1, $F_{(-53/+112)}$]. When RB3 was deleted, there was a strong drop in overall activity and no statistically significant difference in *algD* transcription on LB medium supplemented with 0.3 M NaCl versus LB medium alone and nitrate versus ammonia could be observed (Table 1). These results indicate that RB3 plays a role in the activation of the *algD* promoter and in its response to environmental conditions.

TABLE 1. Effects of deletion of RB3 on the activity of the *algD* promoter in the absence of the far upstream sites RB1 and RB2

Medium[a]	CDO activity[b] of fragment[c]:	
	$F_{(-53/+112)}$ (with RB3)	$F_{(-39/+112)}$ (without RB3)
LB	80 ± 5	31 ± 4
LB + NaCl	158 ± 16	45 ± 7
NH_4	86 ± 10	39 ± 7
NO_3	294 ± 40	52 ± 8

[a] LB, plain LB medium; LB + NaCl, LB supplemented with 0.3 M NaCl; NH_4, minimal medium with 0.2% ammonium sulfate as the nitrogen source; NO_3, minimal medium with 0.2% potassium nitrate as the nitrogen source.

[b] CDO activity was determined in sonic extracts of PAO568 (*muc-2*) grown under conditions as previously described (10, 34). All values expressed as mean milliunits per milligram of protein ± standard error. Extract preparation and enzyme assay were described previously (10, 30). Units are defined in Materials and Methods.

[c] $F_{(-53/+112)}$, fragment extending from −53 to +112 relative to the *algD* mRNA start site (containing RB3); $F_{(-39/+112)}$, fragment extending from −39 to +112 (RB3 deleted). Both fragments were cloned in pVDX18, and the resulting fusions were conjugated into *P. aeruginosa* PAO568.

DNase I footprinting analysis of RB3. In order to precisely map the site of AlgR binding to RB3, as well as to pinpoint the recognition sequence for AlgR within this region, a DNase I footprinting analysis was performed. Conditions used to footprint RB1 and RB2 (29) were not suitable for the footprinting of RB3, most likely because of the weaker nature of protein-DNA interactions at RB3. An optimal set of conditions, as described in Materials and Methods, was formulated to permit the footprinting of RB3. As an additional level of control, DNase I footprinting patterns using two different fragments [$F_{(-144/+11)}$ and $F_{(-80/+11)}$], both containing the putative RB3 site, were compared. End-labeled fragments were generated by cleavage at the *Cla*I site (+11), treatment with phosphatase, phosphorylation with [γ-^{32}P]ATP, and digestion with either *Nsi*I or *Eco*RV. The resulting probes were incubated with AlgR, treated with DNase I, and run next to each other on a sequencing gel. The products of DNase I digestion were run along the side of a sequencing ladder generated using the 16-mer oligonucleotide MO2 (Materials and Methods). The 5′ end of MO2 matched the position within the *Cla*I site that was labeled in footprinting experiments. The use of such an oligonucleotide primer permitted direct comparison of footprinting patterns with the nucleotide sequence of this region generated by using the dideoxynucleotide sequencing method. Typical results of such experiments are shown in Fig. 3. Probes incubated in the presence of AlgR revealed a single discrete area of protection, indicating the presence of a single AlgR-binding site. Furthermore, the position of the observed footprint was identical in both fragments. The location of RB3, mapped by DNase I footprinting analysis, was in agreement with the mapping of RB3 by gel mobility shift DNA binding assays. The position of RB3 was additionally confirmed by hydroxyl radical footprinting analysis (data not shown). The protection pattern observed in DNase I footprinting experiments, which extended over the region spanning positions −50 to −30, had a continuous area of protec-

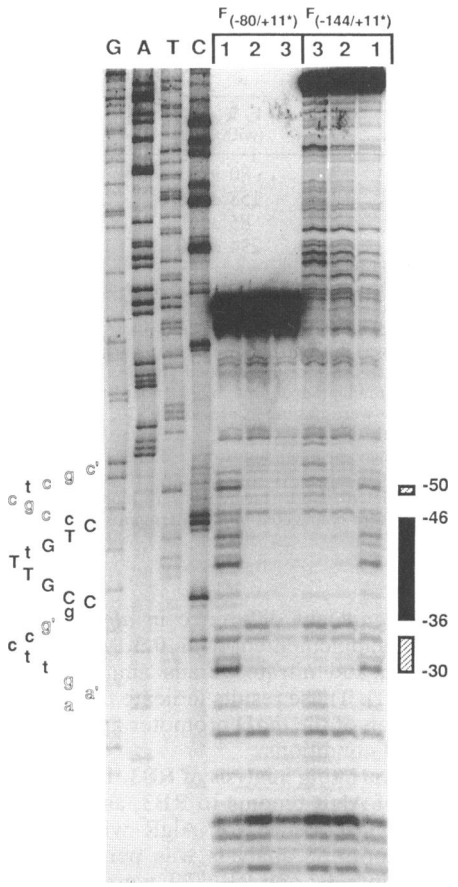

FIG. 3. DNase I footprinting of AlgR bound at RB3. The footprint patterns of two different end-labeled fragments, $F_{(-80/+11^*)}$ and $F_{(-144/+11^*)}$, were compared (the asterisk denotes the labeled end). Lanes: 1, no AlgR added; 2, 1.5 μg of AlgR; 3, 3 μg of AlgR. The G, A, T, and C lanes show the sequencing ladder generated using the oligonucleotide MO2 (5′CGATAGGCATCGCGGT3′). The 5′ end of MO2 matched the position within the *Cla*I site which was labeled in footprinting experiments. This permitted a direct alignment of the nucleotide sequence and the footprinting pattern. Boxes indicate the regions protected from DNase I digestion by AlgR binding. Solid box, continuous region of protection; hatched boxes, additional regions of protection. Bold letters indicate protected nucleotides. Capitalized bold letters are those nucleotides that are identical in all three AlgR-binding sites (RB1, RB2, and RB3). Hypersensitive sites are indicated (′).

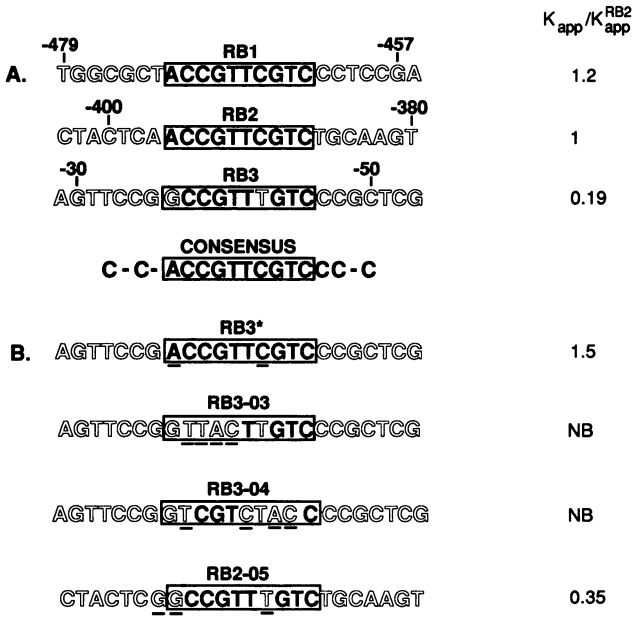

FIG. 4. Nucleotide sequences and relative affinities of AlgR-binding sites within the *algD* promoter. (A) Sequence alignment of the wild-type AlgR-binding sites. Numbers are given relative to the *algD* mRNA start site and denote the boundaries of DNase I protection. All sequences are presented in the 5′-to-3′ direction. Boxed nucleotides represent the core sequence of each AlgR-binding site. The bold letters within the consensus core sequence are those nucleotides conserved in all three or in two of three AlgR-binding sites. Also shown is a consensus sequence of additional conserved nucleotides which are located within the range of all three footprints. (B) Sequences of mutant RB sites. RB3* contains the core of RB2 within the RB3 site. RB3-03 and RB3-04 are two down-mutants of RB3 which no longer bind AlgR. RB2-05 has the RB3 core within the RB2 site. RB2-05 also has a change immediately upstream of the core sequence (G in place of A) which was introduced to facilitate screening by creating a restriction site. This G is also present in RB3. Relative affinities of each site for AlgR are expressed as the ratio of K_{app} for a given site and K_{app} for RB2 ($K_{app}^{RB2} = 13.9 \times 10^6\ M^{-1}$; relative error = 11%); binding of AlgR to RB2 was used as a reference in all experiments. Relative errors in each case varied between 8 and 16%, as determined by the curve-fitting program. NB, no binding.

tion encompassing nucleotides −46 to −36 (Fig. 3). This region contained the sequence 5′gCCGTTtGTC3′ (lowercase letters indicate mismatches with the corresponding positions in the RB1 and RB2 core), which is identical to the core sequence of RB1 and RB2 in 8 of 10 bases. Interestingly, this sequence runs in the direction opposite that of RB1 and RB2. The results of the footprinting analyses presented here demonstrated the presence and determined the location of a third discrete AlgR-binding site within the *algD* promoter and further substantiated the role of the core sequence as a likely recognition site for AlgR (Fig. 4).

Comparison of affinities of AlgR for RB2 and RB3. Gel mobility shift DNA binding assays (29) and a relative difficulty in footprinting RB3 were indicative of a lower affinity of AlgR for RB3. In order to further investigate these observations, the affinities of AlgR for RB2 and RB3 were compared. Figure 5 illustrates the comparison of AlgR binding to RB2 and RB3 in mobility shift DNA binding assay. It is apparent from this gel that concentrations of AlgR which saturate approximately half of the RB2 sites are not sufficient to bind any substantial amount of RB3. Furthermore, concentrations of AlgR which saturate approximately half of the RB3 sites result in almost complete binding of RB2.

To derive more quantitative parameters, titration curves of AlgR binding to fragments containing RB2 or RB3 were generated. In these experiments, the DNA concentration was kept constant and increasing amounts of AlgR were added to the reaction mixture. The distribution of reaction products in the bound and unbound states was analyzed by mobility shift DNA binding assay and quantitated by two-dimensional scanning densitometry. The results of these studies are shown in Fig. 6A. The K_{app}^{RB2} and K_{app}^{RB3} values derived by statistical nonlinear curve-fitting (see Materials and Methods) were 1.39×10^7 and $2.68 \times 10^6\ M^{-1}$, respectively. This translates into the difference in free energy of

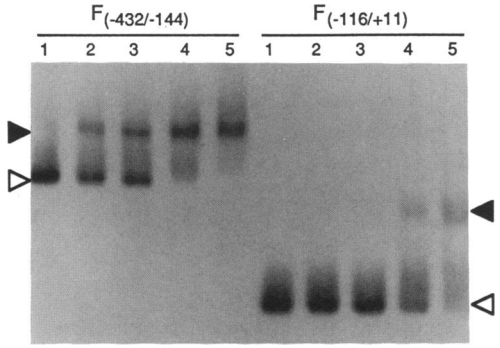

FIG. 5. Comparison of the affinities of AlgR for RB2 and RB3. Two uniformly labeled fragments, $F_{(-432/-144)}$ containing RB2 alone and $F_{(-116/+11)}$ containing RB3 alone (Fig. 1C), were incubated with increasing concentrations of AlgR and analyzed by gel mobility shift DNA binding assay. Lanes in each set: 1, no AlgR; 2, 3, 4, and 5: 7.8, 15.6, 62.5, ng, and 250 ng of AlgR, respectively. Open triangles, unbound radiolabeled fragments: solid triangles, protein-DNA complexes.

AlgR binding to RB2, relative to that of AlgR binding to RB3, of −0.93 kcal/mol (−3.89 kJ/mol), derived as explained in Materials and Methods. This difference is similar in magnitude to the difference in free energy of binding of bacteriophage λ *c*I repressor to the operator sites O_L1 and O_L3 (−1.4 kcal/mol [−5.8 kJ/mol]) (34). These studies established that RB3 was a lower-affinity binding site than RB2. This was in agreement with the finding that although the core sequence of RB3 extensively matched the core sequence of the high-affinity binding sites RB1 and RB2, this similarity was only partial because of the presence of two mismatches of 10 residues.

Role of the core sequence in AlgR binding. The conservation of the core sequence in RB1, RB2, and RB3 suggests that the core sequence is important for AlgR recognition and binding. Such notions were further confirmed by determining K_{app} for RB1, which was found to be 1.66×10^7 M^{-1} (Fig. 6A). This site has no similarity with RB2 outside the core sequence (Fig. 4). K_{app}^{RB1} was very close to the value of K_{app}^{RB2}, the ratio of the two constants being 1.2 (Fig. 4). The difference in free energy of binding between RB1 and RB3 was −1.05 kcal/mol (−4.39 kJ/mol), similar to the difference between RB2 and RB3.

If the two mismatches between cores of RB3 on one side and RB1 and RB2 on the other side were responsible for the reduced affinity of AlgR in the case of RB3, then changing these positions in RB3 to match the core of the upstream sites should result in improved AlgR binding. Conversely, altering the same two nucleotides in RB2 to match the residues found in RB3 should lower the affinity of AlgR for RB2. This hypothesis was tested by using site-directed mutagenesis as described in Materials and Methods. The core sequence of RB3 was altered from 5′gCCGTTtGTC3′ to 5′ACCGTTCGTC3′ (lowercase letters representing the mismatches between RB3 and RB2). This mutated site, termed RB3*, was tested in a quantitative binding assay with AlgR. RB3* displayed significantly enhanced affinity for AlgR, as illustrated in Fig. 7. RB3* had an apparent association constant of 2.11×10^7 M^{-1} (Fig. 6C), which was slightly higher than the value obtained with RB2. Corroborating these findings were the results of the converse experiment, in which the core of RB2 was changed to 5′gCCGTTtGTC3′ (lowercase letters denote departures from the original RB2 core). In this case, one additional nucleotide immediately upstream of the core region has also been changed (Fig. 4B) to facilitate screening of mutants. These changes lowered the affinity of AlgR for the modified RB2 site (termed RB2-05), and the apparent association constant (4.97×10^6 M^{-1}) was closer to that of RB3 (Fig. 6B). These experiments established the role of the difference between RB2 and RB3 cores

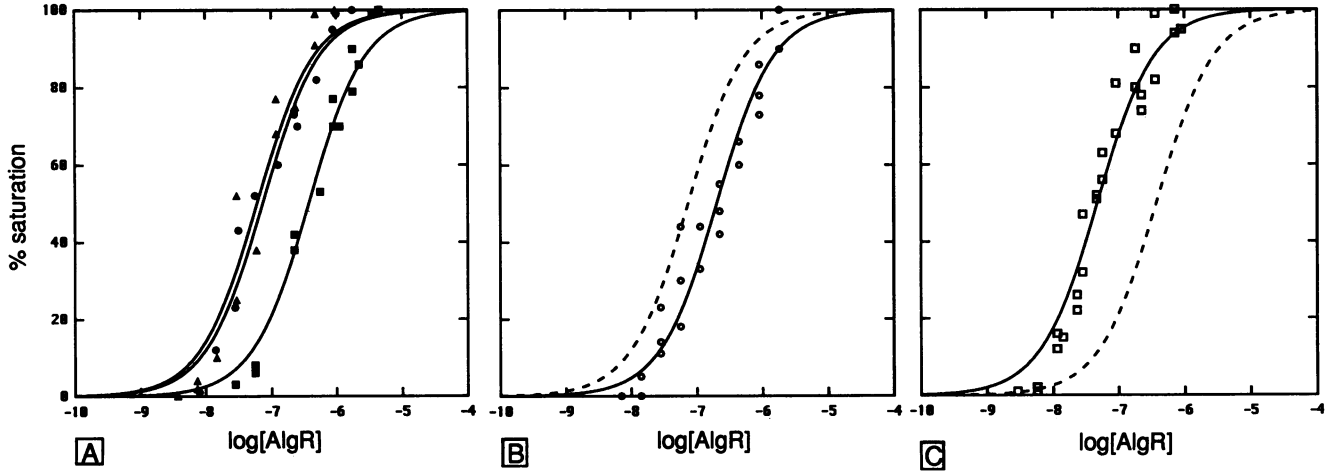

FIG. 6. Titration curves of AlgR binding to RB1, RB2, RB3, and mutant RB2-05 and RB3* sites. Uniformly labeled DNA probes containing RB1 $[F_{(-533/-404)}]$, RB2 $[F_{(-432/-144)}]$, or RB3 $[F_{(-116/+11)}]$ (Fig. 1B) were incubated with increasing amounts of AlgR, and the products were analyzed as described in Materials and Methods (see "Quantitative binding measurements"). The fraction of the bound probe (percent saturation) was plotted as the function of AlgR input expressed as logarithm of its molar concentration in the reaction mixture. (A) Titration curves for wild-type promoters. Solid triangles and the leftmost curve, RB1; solid circles and middle curve, RB2; solid squares and the rightmost curve, RB3. Apparent association constants (K_{app}) were determined by curve fitting to a nonlinear model, as described in Materials and Methods, and were found to be 1.66×10^7 (RB1), 1.39×10^7 (RB2), and 2.68×10^6 (RB3) M^{-1}. (B) Titration curve for RB2-05 (open circles and solid line); dashed line, binding curve for RB2 as in panel A. The K_{app} for RB2-05 was 4.97×10^6 M^{-1} (C) Titration curve for RB3* (open squares and solid line); dashed line, binding curve for RB3 as in panel A. The K_{app} for RB3* was 2.11×10^7 M^{-1}.

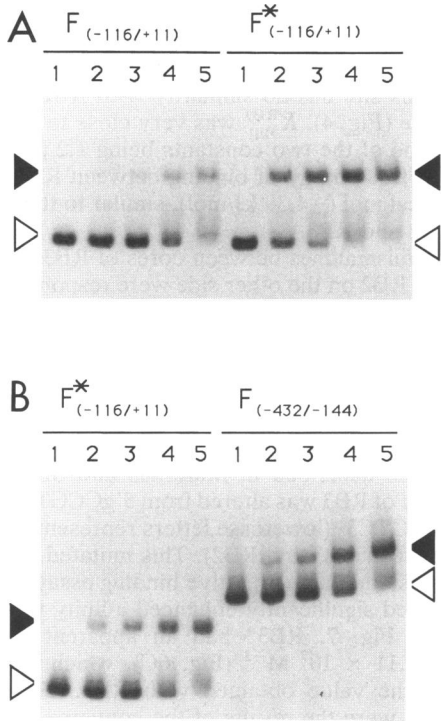

FIG. 7. Comparison of AlgR affinity for RB3* relative to RB3 (A) and RB2 (B) in a mobility shift DNA binding assay. The fragments used are shown in Fig. 1. $F_{(-116/+11)}$ contains RB3 or its mutant RB3* variant (indicated by an asterisk). $F_{(-432/-144)}$ contains RB2. (A) Lanes: 1, no AlgR; 2, 3, 4, and 5, 7.8, 15.6, 62.5, and 250 ng of AlgR, respectively. (B) Lanes: 1, no AlgR; 2, 3, 4, and 5, 3.9, 7.8, 15.6, and 62.5 ng of AlgR, respectively. Open triangles, unbound probe; solid triangles, bound probe.

as the major contributing factor in determining the level of affinity for AlgR.

Additional experiments were performed to examine whether other nucleotides within the core sequence played a role in AlgR binding. This was accomplished by altering 4 nucleotides in two different combinations within the context of RB3 (5′gttacTtGTC3′ and 5′gtCGTctacC3′; lowercase letters denote departure from the high-affinity core sequence such as in RB2). Both of these altered sites (RB3-03 and RB3-04, respectively) no longer bound AlgR (Fig. 8). These experiments confirmed the role of the core sequence as the recognition site for AlgR.

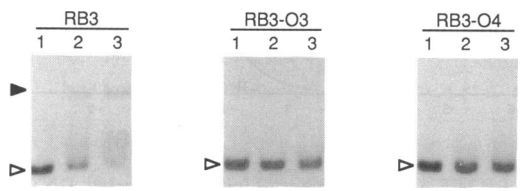

FIG. 8. Loss of AlgR binding activity of mutant RB3 sites when four simultaneous changes of nucleotides are introduced within the core sequence. Two different combinations of substitutions (GttacT TGTC [RB3-03] and GtCGTcTacC [RB3-04]; lowercase letters denote changes relative to the wild-type RB3 sequence) were used. Lanes 1, 2, and 3 contained the amounts of AlgR described in the legend to Fig. 2. Other markings are as described in the legend to Fig. 7.

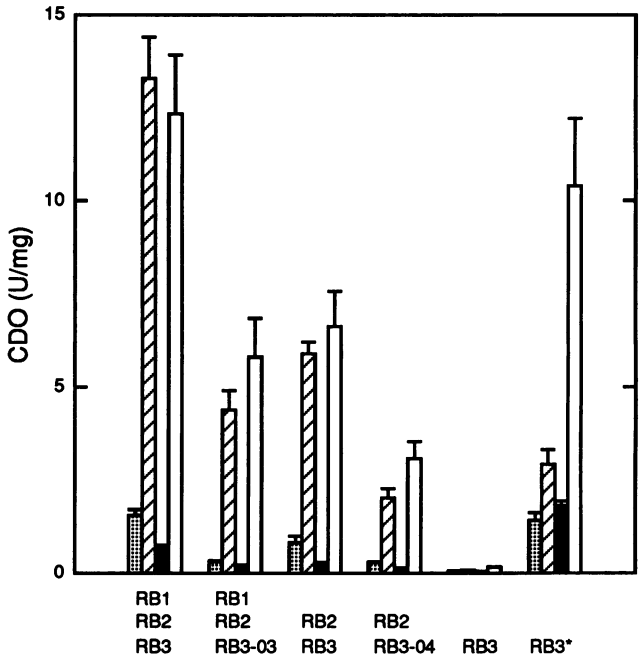

FIG. 9. Effects of point mutations in RB3 on *algD* promoter activity. Different *algD* promoter fragments containing wild-type or mutant sites were assayed for promoter activity using the transcriptional fusion vector pVDX18 (24). CDO (units are defined in Materials and Methods) is the product of *xylE* used as a reporter gene. Growth conditions, extract preparation, and enzyme assays have been described previously (24, 30). Stippled bars, LB medium; hatched bars, LB medium supplemented with 0.3 M NaCl; solid bars, ammonia as the nitrogen source; open bars, nitrate as the nitrogen source. Error bars indicate standard error values. *Hin*dIII-*Eco*RI inserts in pVDX18 were as follows: $F_{(-533/+112)}$, all three sites wild type (RB1, RB2, RB3); $F_{(-533/+112)}$-03, wild-type RB1 and RB2, mutant RB3-03 (RB1, RB2, RB3-03); $F_{(-432/+112)}$, RB1 deleted, wild-type RB2 and RB3 (RB2, RB3); $F_{(-432/+112)}$-04, RB1 deleted, wild-type RB2, mutant RB3-04 (RB2, RB3-04); $F_{(-116/+112)}$, RB1 and RB2 deleted, wild-type RB3 (RB3); and $F_{(-116/+112)}$, RB1 and RB2 deleted, mutant RB3* (RB3*). Numbers in subscripts are defined in the legend to Fig. 1. The sequences of RB3-03, RB3-04, and RB3* are shown in Fig. 4.

Full-size *algD* promoter no longer capable of binding AlgR at RB3 displays lower activity in vivo. Experiments with deletion of RB3 in the context of the minimal *algD* promoter (devoid of the far upstream binding sites RB1 and RB2) indicated that RB3 is functional in vivo. However, the activities observed were more than an order of magnitude lower than activity of the full-size promoter including the RB1, RB2, and RB3 sites (30). To assess a possible participation of RB3 at high levels of *algD* expression, two constructs were compared: (i) a fragment extending from −533 to +112, containing the wild-type RB1, RB2, and RB3 sites, and (ii) the same fragment with a 4-nucleotide change within RB3 (mutant site RB3-03) which no longer binds AlgR at this site (Fig. 8). The numbers of nucleotides and distances between elements were not altered. This construct displayed significantly reduced *algD* promoter activity (Fig. 9). The effect of nonfunctional RB3 was similar in magnitude to the effect when one of the far upstream sites (RB1) was removed. A significant reduction in *algD* promoter activity was also observed (Fig. 9) when a promoter with the RB1 site deleted but containing functional RB2 and RB3 sites was

compared with the same fragment carrying mutant RB3 site (RB3-04). RB3-04, like RB3-03, lost the capacity to bind AlgR (Fig. 8). These experiments indicated that AlgR bound at RB3, in the context of AlgR present at RB1 or RB2, contributes significantly to the activation of *algD*.

The described experiments with deletions and site-directed mutagenesis suggest that AlgR bound at RB3 plays a role as an activator. If this is true, increasing the affinity of RB3 for AlgR should result in an increase in transcriptional activity. To test this hypothesis, a mutant minimal promoter containing RB3* (on a fragment spanning positions −116 to +112 and thus lacking RB1 and RB2) was assayed for activity in vivo. RB3* has improved binding of AlgR, causing it to be equal to or slightly exceeding that of RB2 (Fig. 6C). This resulted in a strong enhancement of *algD* promoter activity relative to the same fragment containing the wild-type RB3 site (Fig. 9). Activity levels of the minimal promoter with RB3* approached, on certain media, the activities of the full-size promoter containing all three wild-type RB1, RB2, and RB3 sites (Fig. 9).

DISCUSSION

In this work, a third AlgR-binding site within the *algD* promoter has been characterized and an unusual overall organization of AlgR-binding sites has been revealed. The newly described site, termed RB3, has been initially delimited using gel mobility shift DNA binding assay and then precisely defined by DNase I footprinting analysis. The role of RB3 in the transcriptional activation of *algD* is supported by deletion analysis, site-directed mutagenesis, and functional assays of the *algD* promoter. A distinct residual activation and environmental modulation of the *algD* promoter, still observable when both of the far upstream sites (RB1 and RB2) are removed, depends on RB3. Moreover, RB3 plays a significant role in the high-level expression of the full-size *algD* promoter, equaling in magnitude the effect of one of the far upstream sites (RB1).

Apparent association constants for different AlgR-binding sites (tabulated in Fig. 4 as ratios relative to K_{app}^{RB2}) have been derived in this work as a quantitative measure of the relative affinities of RB1, RB2, RB3, and mutant sites for AlgR. All three binding sites, RB1, RB2, and RB3, encompass a highly conserved sequence, called the core sequence, which is in each case centered around the middle of the region protected by AlgR from DNase I attack (Fig. 4A). This sequence has been noted initially as a set of direct repeats in the region required for high-level transcription of *algD* (30) and later shown to be within the far upstream AlgR-binding sites (21, 29). Site-directed mutagenesis presented here proves that the core sequence plays a critical role in AlgR recognition. Nevertheless, when the core sequences of all three AlgR-binding sites were aligned, additional conserved nucleotides upstream and downstream of the core sequence were observed within the regions encompassed by the footprints (Fig. 4A). It is possible that these or additional nucleotides contribute to the overall strength of AlgR binding, which could explain minor variations in K_{app} values observed with some mutant sites.

Unlike the previously identified AlgR-binding sites RB1 and RB2 (29), which are located in the far upstream region of the *algD* promoter (30), RB3 is located close to the *algD* mRNA start site. The direction of the core sequence of RB3 is in the opposite orientation to that of the core sequences of RB1 and RB2. The core sequences of the far upstream binding sites RB1 and RB2 represent a set of two perfect direct repeats with periodicity of 76 bp (30). The core sequence of RB3, which is in the opposite orientation to that of RB1 and RB2, is separated from the core sequence of the nearest far upstream site RB2 by 341 bp. Taken together, the three AlgR-binding sites can be viewed as a complex, lopsided palindrome with symmetrical half-sequences separated by a large intervening segment of DNA.

Experiments presented here indicate that AlgR bound at RB1 or RB2 may operate, to a significant degree, independently of AlgR bound at RB3. The direction of AlgR-binding sites may reflect the need for proper orientation of AlgR to enable its interaction with components of the transcription initiation complex. In one model, AlgR bound at RB1 or RB2 may require DNA bending or looping in order to interact with the transcriptional apparatus, similar to the activation of the *nifH* or *glnA* promoter by activators bound at upstream sites (20, 37). If a 180° loop were formed, this would bring AlgR bound at RB1 or RB2 in the same orientation relative to RNA polymerase as AlgR bound at RB3. The proximity and a proper orientation of AlgR at RB3 may help understand how this lower-affinity site contributes to the activation process. Binding of the activator to a lower-affinity site located in the proximity of RNA polymerase may be equivalent in its net effect, under certain conditions, to the binding of AlgR to a much stronger site, but which requires additional steps, such as bending, looping, or diffusion in order to interact with transcriptional apparatus.

Although the far upstream sites appear to be independent of RB3 to a certain degree, it is not possible to absolutely exclude AlgR-AlgR interactions bound to different sites of the *algD* promoter or participation of other factors associating with the intervening DNA. This is based on the finding that RB3, in the absence of the upstream sites, cannot support high-level transcription of *algD*. In this model, compatible with sequential saturation of RB sites which has been observed in vitro (data not shown), RB1 and RB2 are significantly loaded with AlgR prior to any substantial binding of AlgR at RB3. AlgR binding to these sites may be largely independent of RB3. However, once the far upstream sites are loaded with AlgR, this may affect AlgR binding at RB3, possibly via protein-protein interactions, thus making AlgR association with RB3 dependent on the presence of far upstream sites.

Our preliminary attempts to explore potential interactions of unmodified AlgR bound at RB2 with AlgR located at RB3 support the notion that such putative processes are either too weak to be detected by mobility shift DNA binding assay (data not shown) or may be dependent on the phosphorylation state of AlgR or participation of additional regulatory elements. Perhaps related to the inability to observe cooperatively by mobility shift assays is the absence of any significant intrinsic bending of this DNA region (28). Thus, these putative processes, as well as possible interactions of AlgR bound at RB1 or RB2 with RNA polymerase, may either depend on a protein induced DNA bending or looping, such as in the case of NifA-dependent activation of *nifH* (20), or NtrC-dependent activation of *glnA* (37), respectively, or other factors determining local and global nucleoid structure. On the basis of independent genetic studies, it is known that other elements, such as the histone-like protein AlgP (Hp1), can enhance activity of the *algD* promoter (11, 13, 22, 24). In addition, the *algD* promoter has several sequences resembling integration host factor (IHF) binding sites (28). We have shown that polyclonal antibodies against *E. coli* IHF recognize a polypeptide with a similar M_r in crude *P. aeruginosa* extracts and, more importantly, that

IHF binds to the *algD* promoter and causes a significant bending of DNA (28). Experiments are in progress to examine whether protein-induced bending can facilitate footprints of AlgR at RB3 when RB1 and RB2 are present on the same fragment. Another important aspect of *algD* promoter regulation that needs to be explored is whether and how phosphorylation of AlgR affects its interaction with different binding sites. It is possible that a phosphorylation of AlgR typical of the two-component systems, which has been recently demonstrated (13a, 25) using a heterologous kinase CheA (35), could play a pivotal role in the recruitment of sites and may guide the macromolecular assembly and its activity at the *algD* promoter.

The peculiar organization (4) of the *algD* promoter reported here, in conjunction with the control by multiple signal transduction systems and histone-like elements, involving AlgR (29), AlgB (17, 39), AlgP (Hp1) (11, 13, 22), AlgQ (12, 24), and potentially other factors, is a further step toward delineation of the regulation of mucoidy. It is also an example of the elaborate regulatory networks necessary to control such complex phenotypes as the expression of virulence determinants.

ACKNOWLEDGMENTS

We thank S. Sonsteby for help with transcriptional fusion assays.

This work was supported by grant AI31139 from the National Institutes of Health, grant G229 from the Cystic Fibrosis Foundation, and in part by grant DMB-8807424 from the National Science Foundation. C.D.M. was supported in part by training grant T32 AI07272-06 from the National Institutes of Health and by Predoctoral Traineeship grant 5405 from the Cystic Fibrosis Foundation.

REFERENCES

1. **Ausubel, F. M., R. Brent, R. E. Kingston, D. D. Moore, J. G. Seidman, J. A. Smith, and K. Struhl.** 1989. Current protocols in molecular biology. John Wiley & Sons, Inc., New York.
2. **Bauer, C. E., S. D. Hesse, D. A. Waechter-Brulla, S. P. Lynn, R. I. Gumport, and J. F. Gardner.** 1985. A genetic enrichment for mutations constructed by oligodeoxynucleotide-directed mutagenesis. Gene **37**:73–81.
3. **Bradford, M. M.** 1976. A rapid and sensitive method for the quantitation of microgram quantities of protein utilizing the principle of protein-dye binding. Anal. Biochem. **72**:245–254.
4. **Branden, C., and J. Tooze.** 1991. Introduction to protein structure. Garland Publishing, Inc., New York.
5. **Brenowitz, M., D. F. Senear, M. A. Shea, and G. K. Ackers.** 1986. "Footprint" titrations yield valid thermodynamic isotherms. Proc. Natl. Acad. Sci. USA **83**:8462–8466.
6. **Codosh, L. A., R. W. Carthew, and P. A. Sharp.** 1986. A single polypeptide possesses the binding and transcription activities of the adenovirus major late transcription factor. Mol. Cell. Biol. **6**:4723–4733.
7. **Deretic, V., R. Dikshit, W. M. Konyecsni, A. M. Chakrabarty, and T. K. Misra.** 1989. The *algR* gene, which regulates mucoidy in *Pseudomonas aeruginosa*, belongs to a class of environmentally responsive genes. J. Bacteriol. **171**:1278–1283.
8. **Deretic, V., J. F. Gill, and A. M. Chakrabarty.** 1987. Gene *algD* coding for GDPmannose dehydrogenase is transcriptionally activated in mucoid *Pseudomonas aeruginosa*. J. Bacteriol. **169**:351–358.
9. **Deretic, V., J. F. Gill, and A. M. Chakrabarty.** 1987. *Pseudomonas aeruginosa* infections in cystic fibrosis: nucleotide sequence and transcriptional regulation of the *algD* gene. Nucleic Acids Res. **15**:4567–4581.
10. **Deretic, V., J. R. W. Govan, W. M. Konyecsni, and D. W. Martin.** 1990. Mucoid *Pseudomonas aeruginosa* in cystic fibrosis: mutations in the *muc* loci affect transcription of the *algR* and *algD* genes in response to environmental stimuli. Mol. Microbiol. **4**:189–196.
11. **Deretic, V., N. S. Hibler, and S. C. Holt.** 1992. Immunocytochemical analysis of AlgP (H_p1), a histonelike element participating in control of mucoidy in *Pseudomonas aeruginosa*. J. Bacteriol. **174**:824–831.
12. **Deretic, V., and W. M. Konyecsni.** 1989. Control of mucoidy in *Pseudomonas aeruginosa*: transcriptional regulation of *algR* and identification of the second regulatory gene, *algQ*. J. Bacteriol. **171**:3680–3688.
13. **Deretic, V., and W. M. Konyecsni.** 1990. A prokaryotic regulatory factor with a histone H1-like carboxy-terminal domain: clonal variation of repeats within *algP*, a gene involved in regulation of mucoidy in *Pseudomonas aeruginosa*. J. Bacteriol. **172**:5544–5554.

13a. **Deretic, V., J. H. J. Leveau, C. D. Mohr, and N. S. Hibler.** 1992. *In vitro* phosphorylation of AlgR, a regulator of mucoidy in *Pseudomonas aeruginosa*, by a histidine protein kinase and effects of small phospho-donor molecules. Mol. Microbiol. **6**:2761–2767.

14. **Deretic, V., C. D. Mohr, and D. W. Martin.** 1991. Mucoid *Pseudomonas aeruginosa* in cystic fibrosis: signal transduction and histone-like elements in the regulation of bacterial virulence. Mol. Microbiol. **5**:1557–1583.
15. **DeVault, J. D., K. Kimbara, and A. M. Chakrabarty.** 1990. Pulmonary dehydration and infection in cystic fibrosis: evidence that ethanol activates alginate gene expression and induction of mucoidy in *Pseudomonas aeruginosa*. Mol. Microbiol. **4**:737–745.
16. **Fried, M., and D. M. Crothers.** 1981. Equilibria and kinetics of *lac* repressor-operator interactions by polyacrylamide gel electrophoresis. Nucleic Acids Res. **9**:6505–6525.
17. **Goldberg, J. B., and T. Dahnke.** 1992. *Pseudomonas aeruginosa* AlgB, which modulates the expression of alginate, is a member of the NtrC subclass of prokaryotic regulators. Mol. Microbiol. **6**:59–66.
18. **Govan, J. R. W.** 1988. Alginate biosynthesis and other unusual characteristics associated with the pathogenesis of *Pseudomonas aeruginosa* in cystic fibrosis. p. 67–96. *In* E. Griffiths, W. Donachie, and J. Stephen (ed.), Bacterial infections of respiratory and gastrointestinal mucosae. IRL Press, Oxford.
19. **Hoiby, N., G. Doring, and P. O. Schiotz.** 1987. Pathogenic mechanisms of chronic *Pseudomonas aeruginosa* infections in cystic fibrosis patients. Antibiot. Chemother. **39**:60–76.
20. **Hoover, T. R., E. Santero, S. Porter, and S. Kustu.** 1990. The integration host factor stimulates interaction of RNA polymerase with NifA, the transcriptional activator for nitrogen fixation operons. Cell **63**:11–22.
21. **Kato, J., and A. M. Chakrabarty.** 1991. Purification of the regulatory protein AlgR1 and its binding in the far upstream region of the *algD* promoter in *Pseudomonas aeruginosa*. Proc. Natl. Acad. Sci. USA **88**:1760–1764.
22. **Kato, J., T. K. Misra, and A. M. Chakrabarty.** 1990. AlgR3, a protein resembling eukaryotic histone H1, regulates alginate synthesis in *Pseudomonas aeruginosa*. Proc. Natl. Acad. Sci. USA **87**:2887–2891.
23. **Konyecsni, W. M., and V. Deretic.** 1989. Broad-host-range plasmid and M13 bacteriophage-derived vectors for promoter analysis in *Escherichia coli* and *Pseudomonas aeruginosa*. Gene **74**:375–386.
24. **Konyecsni, W. M., and V. Deretic.** 1990. DNA sequence and expression analysis of *algP* and *algQ*, components of the multigene system transcriptionally regulating mucoidy in *Pseudomonas aeruginosa*: *algP* contains multiple direct repeats. J. Bacteriol. **172**:2511–2520.
25. **Leveau, J. H. J., and V. Deretic.** Unpublished data.
26. **Marquardt, D. W.** 1963. An algorithm for least squares estimation of nonlinear parameters. J. Soc. Ind. Appl. Math. **11**:431–441.
27. **May, T. B., D. Shinaberger, R. Maharaj, J. Kato, L. Chu, J. D. DeVault, S. Roychoudhury, N. A. Zielenski, A. Berry, R. K. Rothmel, T. K. Misra, and A. M. Chakrabarty.** 1991. Alginate synthesis by *Pseudomonas aeruginosa*: a key pathogenic factor in chronic pulmonary infections in cystic fibrosis. Clin. Microbiol. Rev. **4**:191–206.
28. **Mohr, C. D., and V. Deretic.** Unpublished data.

29. **Mohr, C. D., N. S. Hibler, and V. Deretic.** 1991. AlgR, a response regulator controlling mucoidy in *Pseudomonas aeruginosa*, binds to the FUS sites of the *algD* promoter located unusually far upstream from the mRNA start site. J. Bacteriol. **173:**5136–5143.
30. **Mohr, C. D., D. W. Martin, W. M. Konyecsni, J. R. W. Govan, S. Lory, and V. Deretic.** 1990. Role of the far-upstream sites of the *algD* promoter and the *algR* and *rpoN* genes in environmental modulation of mucoidy in *Pseudomonas aeruginosa*. J. Bacteriol. **172:**6576–6580.
31. **Ohman, D. E., J. B. Goldberg, and J. L. Flynn.** 1990. Molecular analysis of the genetic switch activating alginate production. *In* S. Silver, A. M. Chakrabarty, B. Iglewski, and S. Kaplan (ed.), *Pseudomonas* biotransformations, pathogenesis, and evolving biotechnology. American Society for Microbiology, Washington, D.C.
32. **Pier, G. B., G. J. Small, and H. B. Warren.** 1990. Protection against mucoid *Pseudomonas aeruginosa* in rodent models of endobronchial infections. Science **249:**537–540.
33. **Roychoudhury, S., T. B. May, S. K. Singh, D. S. Feingold, and A. M. Chakrabarty.** 1989. Purification and characterization of guanosine diphospho-D-mannose dehydrogenase. J. Biol. Chem. **264:**9380–9385.
34. **Senear, D. F., M. Brenowitz, M. A. Shea, and G. K. Ackers.** 1986. Energies of cooperative protein-DNA interactions: comparison between quantitative deoxyribonuclease footprint titration and filter binding. Biochemistry **25:**7344–7354.
35. **Stock, J. B., A. J. Ninfa, and A. M. Stock.** 1989. Protein phosphorylation and the regulation of adaptive responses in bacteria. Microbiol. Rev. **53:**450–490.
36. **Studier, F. W., and B. A. Moffat.** 1986. Use of bacteriophage T7 RNA polymerase to direct selective high-level expression of cloned genes. J. Mol. Biol. **189:**113–130.
37. **Su, W., S. Porter, S. Kustu, and H. Echols.** 1990. DNA-looping and enhancer activity: association between DNA-bound NtrC activator and RNA polymerase at the bacterial *glnA* promoter. Proc. Natl. Acad. Sci. USA **87:**5504–5508.
38. **Vandeyar, M. A., M. P. Weiner, C. J. Hutton, and C. A. Batt.** 1988. A simple and rapid method for the selection of oligodeoxynucleotide-directed mutants. Gene **65:**129–133.
39. **Wozniak, D. J., and D. E. Ohman.** 1991. *Pseudomonas aeruginosa* AlgB, a two-component response regulator of the NtrC family, is required for *algD* transcription. J. Bacteriol. **173:** 1406–1413.